



1 **The long-term trend and production sensitivity change of the U.S. ozone pollution from**
2 **observations and model simulations**

3

4 Hao He^{1,2}, Xin-Zhong Liang^{1,2}, Chao Sun¹, Zhining Tao^{3,4}, and Daniel Q. Tong^{1,5}

5 ¹Department of Atmospheric and Oceanic Science, University of Maryland, College Park,
6 Maryland 20742, USA

7 ²Earth System Science Interdisciplinary Center, University of Maryland, College Park, Maryland
8 20740, USA

9 ³Universities Space Research Association, Columbia, Maryland 21046, USA

10 ⁴NASA Goddard Space Flight Center, Greenbelt, Maryland 20771, USA

11 ⁵Center for Spatial Information Science and Systems, George Mason University, Fairfax, VA
12 22030, USA

13

14 **Keywords:** Air Quality Trend, CMAQ Simulations, Ozone Production Sensitivity

15

16 Corresponding to Dr. Xin-Zhong Liang (xliang@umd.edu)

17



18 **Abstract**

19 We investigated the ozone pollution trend and its sensitivity to key precursors from 1990
20 to 2015 in the United States using long-term EPA AQS observations and mesoscale simulations.
21 The modeling system, a coupled regional climate – air quality (CWRf-CMAQ) model, well
22 captured summer surface ozone pollution during the past decades, having a mean slope of linear
23 regression with AQS observations at ~ 0.75 . While the AQS network has limited spatial coverage
24 and measures only a few key chemical species, the CWRf-CMAQ provides comprehensive
25 simulations to enable a more rigorous study of the change in ozone pollution and chemical
26 sensitivity. Analysis of seasonal variations and diurnal cycle of ozone observations showed that
27 peak ozone concentrations in the summer afternoon decreased ubiquitously across the United
28 States, up to 0.5 ppbv/yr in major non-attainment areas such as Los Angeles, while
29 concentrations at other hours such as the early morning and late afternoon increased slightly.
30 Consistent with the AQS observations, CMAQ simulated a similar decreasing trend of peak
31 ozone concentrations in the afternoon, up to 0.4 ppbv/yr, and increasing ozone trends in the early
32 morning and late afternoon. While a monotonic decreasing trend (up to 0.5 ppbv/yr) in the odd
33 oxygen ($O_x = O_3 + NO_2$) concentrations are simulated by CMAQ at all daytime hours. This result
34 suggests that the increased ozone in the early morning and late afternoon was likely caused by
35 reduced NO-O₃ titration driven by continuous anthropogenic NO_x emission reductions in the past
36 decades. Furthermore, the CMAQ simulations revealed a shift in chemical regimes of ozone
37 photochemical production. From 1990 to 2015, surface ozone production in some metropolitan
38 areas, such as Baltimore, has transited from VOC-sensitive environment (>50% probability) to
39 NO_x-sensitive regime. Our results demonstrated that the long-term CWRf-CMAQ simulations
40 can provide detailed information of the ozone chemistry evolution under a changing climate, and



41 may partially explain the U.S. ozone pollution responses to regional and national regulations.

42

43 **1. Introduction**

44 Tropospheric ozone (O_3) is one of the major air pollutants, regulated by the U.S.
45 Environmental Protection Agency (EPA), that pose myriad threats to public health and the
46 environment (Adams et al., 1989; WHO, 2003; Ashmore, 2005; Anderson, 2009; Jerrett et al.,
47 2009). It is also an important greenhouse gas due to the absorption of thermal radiation, affecting
48 the climate (Fishman et al., 1979; Ramanathan and Dickinson, 1979; IPCC, 2013). The major
49 source of tropospheric ozone is photochemical production from ozone precursors such as carbon
50 monoxide (CO), volatile organic compounds (VOCs), and nitrogen oxides (NO_x) at the presence
51 of sunlight (Crutzen, 1974; Seinfeld, 1991; Jacob, 2000; EPA, 2006), while downward transport
52 of stratospheric air mass contributes substantially to ozone concentrations in upper troposphere
53 (Levy et al., 1985; Holton et al., 1995; Stevenson et al., 2006). In the past decades, ozone
54 pollution in the United States has been reduced substantially due to regulations on anthropogenic
55 emissions of ozone precursors (Oltmans et al., 2006; Lefohn et al., 2008, 2010; Cooper et al.,
56 2012; He et al., 2013; Cooper et al., 2014), although some studies suggested no trend or slight
57 increases at some rural areas (Jaffe and Ray, 2007; Lefohn et al., 2010; Cooper et al., 2012).
58 Most of these analyses focused on peak ozone concentrations, e.g., daily maximum 8-hour
59 average ozone (MDA8), during summer, but studies on trends in seasonal and diurnal patterns of
60 ozone pollution are limited. He et al. (2019) analyzed measurements from four monitoring sites
61 in the eastern United States and found different ozone trends between rural and urban sites from
62 the late 1990s to the early 2010s including some increases at certain hours, suggesting effects of
63 national regulations could be regionally dependent. Thus, it is important to extend our study to



64 other regions of the United States in a longer time period.

65 The non-monotonic trends in United States ozone pollution could be caused by the
66 complex non-linear chemistry of ozone production involving NO_x and VOCs (Logan et al., 1981;
67 Finlayson-Pitts and Pitts, 1999; Seinfeld and Pandis, 2006). With continuous reduction of
68 anthropogenic emissions of ozone precursors mainly NO_x and VOCs in the United States, we
69 need to better understand the photochemical regime change for local ozone production (i.e.,
70 ozone production sensitivity), because air pollution regulations could have different effects under
71 NO_x -sensitive and VOC-sensitive environment (Dodge, 1987; Kleinman, 1994). For instance,
72 under a VOC-sensitive photochemical regime, the decrease of NO_x emissions has limited
73 impacts on improving ozone pollution. Previous studies have developed photochemical
74 indicators to identify the ozone production sensitivity (Sillman, 1995; Sillman et al., 1997;
75 Tonnesen and Dennis, 2000b, a; Sillman and He, 2002). Sillman (1999) found the ratio of VOCs
76 and NO_x (VOC/NO_x) has a typical value less than 4 for the VOC-sensitive environment and
77 higher than 15 for the NO_x -sensitive regime. Observation-based studies of ozone production
78 sensitivity relied on research grade measurements of ozone precursors and photochemical
79 intermediates that are not routinely measured by air quality management agencies such as the
80 U.S. EPA. These species include reactive nitrogen compounds (NO_y), nitric acid (HNO_3), and
81 hydrogen peroxide (H_2O_2), normally observed during field campaigns (e.g., Shon et al., 2007;
82 Peng et al., 2011) which only covered limited areas in certain periods. Studies based on air
83 quality models (AQM) could identify the ozone production regimes at regional scales (Sillman et
84 al., 1997; Sillman and He, 2002; Zhang et al., 2009a; Zhang et al., 2009b; Xie et al., 2011), but
85 the simulation periods were usually short (less than one year) and thus could not capture the
86 long-term change in ozone production sensitivity.



87 Regional AQMs are widely used for investigating the U.S. air quality (Tagaris et al.,
88 2007; Tang et al., 2009; Hogrefe et al., 2011; Pour-Biazar et al., 2011; He et al., 2016a; He et al.,
89 2018). They incorporate finer resolutions, more detailed emissions, and more explicit chemical
90 mechanism than global chemical transport models to better resolve characteristics of
91 tropospheric and surface dynamics, physical and chemical processes essential for air quality. Our
92 group has developed and used coupled regional climate-air quality models to study air quality
93 variations under a changing regional climate (Huang et al., 2007; Zhu and Liang, 2013; He et al.,
94 2016a; He et al., 2018). Our previous studies showed the model's ability to capture the decadal
95 U.S. air quality change (e.g., Zhu and Liang, 2013). In this study, we coupled the latest Climate-
96 Weather Research Forecast (CWRF) and the EPA Community Multiscale Air Quality (CMAQ)
97 models. CWRF has demonstrated substantial improvement in downscaling regional climate and
98 extremes (Liang et al., 2012; Chen et al., 2016; Liu et al., 2016a; Liang et al., 2019a; Sun and
99 Liang, 2019a; Sun and Liang, 2019b) and thus can provide more realistic weather conditions for
100 AQMs to produce more credible air quality simulations.

101 To supplement the limited observations in both spatial coverage and chemical species, we
102 conducted a continuous 26-yr CWRF-CMAQ simulation from 1990 to 2015 for a more rigorous
103 analysis of long-term U.S. ozone trend. The model performance of the U.S. air quality was first
104 evaluated against gridded ozone observations. The ozone seasonal variations and diurnal cycles
105 were then extracted to determine the observed long-term trend. The model simulations were
106 subsequently analyzed to explain the observed ozone trends and change in ozone production
107 sensitivity.



108 **2. Observations and model simulations**

109 **2.1 Long-term EPA observations**

110 Hourly measurements of surface ozone concentrations from 1990 to 2015 were available
111 from the EPA Air Quality System (AQS) database ([https://www.epa.gov/outdoor-air-quality-](https://www.epa.gov/outdoor-air-quality-data)
112 [data](https://www.epa.gov/outdoor-air-quality-data)). They have been examined following the EPA guidance including the quality assurance and
113 quality control. The locations and durations of AQS monitoring sites have changed substantially
114 due to logistics and requirements to cover the regions sensitive to air pollution. Figure 1 shows
115 that more than 2000 sites reported ozone measurements from 1990 to 2015. To alleviate the
116 impacts from missing data and short durations, we selected 640 sites that had ozone observation
117 records longer than 20 years. Hourly ozone observations were processed following the approach
118 described in He et al. (2019) to create the long-term seasonal and diurnal records for these
119 stations.

120

121 **2.2 Regional climate modeling**

122 CWRF (Liang et al., 2012) was driven by the European Centre for Medium-Range
123 Weather Forecasts ERA-Interim reanalysis (ERI, Dee et al., 2011) to downscale regional climate
124 variations during 1989-2015 with the first year as the spin-up and not used. We adopted the well-
125 established North American domain with a 30-km grid spacing (Fig. 1), covering the Contiguous
126 United States (CONUS) and neighboring southern Canada, northern Mexico and adjacent
127 oceans. The CWRF incorporated advanced representations of key physical processes and
128 integrations of external forcings crucial to climate scales (Liang et al., 2012). It has been
129 vigorously tested in North America and Asia showing outstanding performance to capture
130 regional climate characteristics (Yuan and Liang, 2011; Qiao and Liang, 2015; Chen et al., 2016;



131 Liu et al., 2016b; Qiao and Liang, 2016; Liang et al., 2019b). The CWRP downscaling has been
132 shown to provide realistic meteorological fields and regional climate signals that can be cordially
133 used to drive the CMAQ for long air quality simulations. Major CWRP physics configurations
134 include the semi-empirical cloudiness parameterization of Xu and Randall (1996), the cloud
135 microphysics scheme of Tao et al. (1989), the short wave and long wave radiation scheme of
136 Chou et al. (2001), the ensemble cumulus parameterization (Qiao and Liang, 2015, 2016; Qiao
137 and Liang, 2017), and the planetary boundary layer scheme of Holtslag and Boville (1993).
138 Hourly CWRP outputs were processed using a modified Meteorology-Chemistry Interface
139 Processor (MCIP, version 4.3) for CMAQ simulations.

140

141 **2.3 Emissions preparation**

142 To prepare anthropogenic emissions, we chose 2014 as the baseline year. This year's
143 emissions were modified from the National Emissions Inventory 2011 (NEI2011). The
144 modifications was based on measurements from the Ozone Monitoring Instrument (OMI)
145 onboard satellite Aura, the ground-based AQS network, and the *in-situ* continuous emissions
146 monitoring in power plants (Tong et al., 2015; Tong et al., 2016). The so modified NEI2011
147 inventory was processed using the Sparse Matrix Operator Kernel Emissions (SMOKE) version
148 3.7 (Houyoux et al., 2000). Emissions from on-road, off-road, and area sources were placed at
149 the model layer closest to the surface. Emissions from point sources, e.g., stacks from power
150 plants, were distributed vertically based on stack height and plume rise. The plume rise was
151 estimated based on the method in Briggs (1972). The inventory pollutants were speciated
152 according to the carbon bond chemical mechanism version 5 (CB05) and AERO5 aerosol
153 mechanism. To fill the gap where NEI2011 data were not available, the Emissions Database for



154 Global Atmospheric Research (EDGAR v3, <http://edgar.jrc.ec.europa.eu/>) at a $1^\circ \times 1^\circ$ resolution
155 developed by the Joint Research Centre of European Commission was adapted. Figure 2 shows
156 an example of 2010-2015 mean NO_x emissions distribution over the modeling domain. Daily
157 mean NO_x emissions have high values in urban areas of cities such as Los Angeles, Chicago, and
158 the northeast corridor from Washington D.C. to Boston.

159 To project emissions from the baseline year into all individual years, we used the scaling
160 factors from Air Pollutant Emissions Trends Data compiled by the U.S. EPA
161 (<https://www.epa.gov/air-emissions-inventories/air-pollutant-emissions-trends-data>). Figure 3
162 shows the emission evolution from 1990 to 2015. Since 1990 anthropogenic emissions of NO_x ,
163 CO, sulfur dioxide (SO_2), and VOCs had steady decreasing trends, with SO_2 experiencing the
164 largest reduction. On the other hand, anthropogenic $\text{PM}_{2.5}$ and NH_3 emissions stayed mostly flat
165 since the early 2000s.

166 The wildfire emissions were based on the Global Fire Emissions Database, Version 4 with
167 small fires (GFEDv4s, Randerson et al., 2017; van der Werf et al., 2017). The $0.25^\circ \times 0.25^\circ$
168 degree resolution GFEDv4s data were projected onto the modeling domain and speciated into the
169 CB05 and AERO5 species. GFEDv4s had a monthly resolution from 1997 to 2000 and daily
170 resolution from 2000 onward. Figure 4 illustrates the fire emissions evolution during 1990 to
171 2015 relative to 2014. Fire emissions have large interannual variations, with high emissions in
172 1998, 2002, 2013, and 2015, and low emissions in 2001, 2004, and 2014. We developed a
173 method to merge the aforementioned anthropogenic and wildfire emissions into the
174 temporalized, gridded and speciated data ready for CMAQ.

175 The biogenic emissions were calculated online within CMAQ based on the Biogenic
176 Emissions Landuse Database, Version 3 (BELD3, <https://www.epa.gov/air-emissions->



177 [modeling/biogenic-emissions-landuse-database-version-3-beld3](#)). The 1-km resolution BELD3
178 data with spatial distribution of 230 vegetation classes over the North America were processed
179 through the Spatial Allocator developed by the Community Modeling and Analysis System
180 (CMAS) center (<https://www.cmascenter.org/sa-tools/>) to generate the gridded vegetation
181 distribution over the study domain. Table 1 lists the 5-yr mean variations of daily major ozone
182 precursor (CO, NO_x, and NMVOCs) emissions in the modeling domain and five subdomains.
183 The emission data show regionally dependent reductions. For instance, compared with 2000-
184 2004, the NO_x emissions in 2005-2009 decreased by ~36% averaged in the CONUS, while 38%
185 and 35% reductions existed in states of California and Texas.

186

187 **2.4 Air quality modeling**

188 The EPA CMAQ model version 5.2 (EPA, 2017) was selected to simulate the U.S. air
189 quality variations driven by CWRM meteorological fields (Section 2.2) and constructed emissions
190 (Section 2.3). Major chemical mechanisms include the Carbon Bond 6 revision 3 (CB6r3) gas
191 phase chemical scheme with updated secondary organic aerosol (SOA) and nitrate chemistry
192 (Yarwood et al., 2010) and the latest AERO6 aerosol scheme (EPA, 2017), which improved U.S.
193 air quality simulations over previous chemical mechanisms (Appel et al., 2016). Chemical initial
194 and boundary conditions were obtained from the default concentration profiles built in CMAQ
195 (EPA, 2017). Simulations were conducted continuously for each 5-year segment (e.g., 1990-
196 1994, 1995-1999, etc.) with two-week spin-up in December prior to each starting years to speed
197 up simulation turn around. Hourly concentrations of ozone and its key precursors such as nitric
198 oxide (NO) and nitrogen dioxide (NO₂) were saved for subsequent analyses.



199 **3. Results**

200 **3.1 Evaluation of CMAQ performance**

201 Our previous studies showed that the direct comparison of observation data from
202 monitoring sites and CMAQ results in 30-km grid could introduce inconsistency for evaluating
203 the model performance (He et al., 2016a). So we applied the EPA Remote Sensing Information
204 Gateway (RSIG) software (available at <https://www.epa.gov/rsig>) to map the site observations
205 onto our CMAQ grid. Figure 5 compares summer (JJA) mean MDA8 ozone in 2014 between
206 gridded AQS observations and CMAQ outputs and shows that the model can well capture the
207 U.S. ozone pollution, except underestimation in urban areas such as the Los Angeles basin.

208 Table 2 summarized the statistics for CMAQ performance of the summer ozone
209 concentrations during 2000 - 2015 in CONUS and subdomains. Linear regression analyses of
210 MDA8 ozone result in a mean slope value of 0.75 for CONUS, i.e., CMAQ slightly
211 underestimates ozone over the United States. In subdomains, CMAQ performance exhibits large
212 interannual variations. For instance, in Texas the linear regression slope and correlation
213 coefficient ranges from 0.58 to 0.97 and 0.55 to 0.86, respectively. Generally, this modeling
214 system has substantially improved performance in the Southeast, California and Texas, and
215 moderately improved performance in the Northeast and Midwest as compared with our previous
216 study (He et al., 2016a). These results demonstrate the ability of CWRf-CMAQ to credibly
217 simulate historical air quality.

218

219 **3.2 Long-term ozone trend in AQS observations**

220 We applied a box-averaging technique (He et al., 2016b; He et al., 2019) to analyze ozone
221 measurements at the selected AQS monitoring sites (Fig 1). This approach used an hour by



222 month box to calculate the mean 24-hr diurnal cycle of ozone for each month. Then we
223 calculated the climatology mean over 24 hours by 12 months and the respective anomaly for
224 each month at each AQS site. Figure 6 shows samples of long-term mean ozone concentrations
225 and anomalies at four non-attainment cities: Baltimore, Maryland; Los Angeles, California;
226 Denver, Colorado; and New York City (NYC), New York. The hour by month climatology (left
227 column of Fig. 6) shows that the peak ozone concentrations in the afternoon during the ozone
228 season (April to September) have been reduced significantly in these cities. However, ozone
229 concentrations in the morning (8 am to 12 pm, all local time hereafter) and at night (8 pm to 8
230 am) increased slightly. These results confirm the effectiveness of recent emission controls which
231 were designed to reduce the peak ozone. But the expansion of ozone at moderate levels (40-50
232 ppbv), which are higher than the natural background of U.S. ozone (Fiore et al., 2002; Fiore et
233 al., 2003; Wang et al., 2009; Lefohn et al., 2014), could cause negative health impacts.

234 The anomaly (right column of Fig. 6) shows large variabilities of ozone concentrations
235 because the ozone production is significantly impacted by regional climate (e.g., temperature,
236 precipitation) with interannual and decadal variations. Large ozone reduction occurred after 2003
237 when the EPA NO_x State Implementation (SIP) call was implemented (He et al., 2013). The
238 anomalies at Los Angeles (Fig. 6b) and NYC (Fig. 6d) shows decreases of the peak ozone in the
239 afternoon of summer and increases in other times and seasons. For Baltimore and Denver, the
240 peak ozone was not monotonically reduced, but increased in some years after 2002. Given the
241 continuous reduction of anthropogenic emissions in the past decades, the increased ozone
242 pollution in these areas could be caused by other factors such as higher summer temperatures in
243 certain years or enhanced stratosphere-troposphere exchange (for Denver at the high altitude
244 area), which need further investigations in the future.



245 We used the linear regression analysis to calculate the slope, correlation (R), and p-value
246 of ozone trend at each local hour. Figure 7 shows ozone trends (slope, unit of ppbv/yr) at AQS
247 sites which are statistically significant ($R^2 > 0.5$, and $p < 0.05$) in the early morning (8 am), at
248 noon (12 pm), in the afternoon (4 pm), and in the evening (8 pm). Consistent results with the
249 four cities (Fig. 6) are found ubiquitously. The peak ozone at noon and in the afternoon generally
250 had a decreasing trend in CONUS, up to 0.5 ppbv/yr, confirming the improved air quality due to
251 regulations, while ozone in the early morning and late afternoon increased slightly at most of
252 monitoring sites. However, AQS sites in the Bay area (San Francisco, California) and Denver
253 had stronger positive trends in the day time. The possible explanations include the trans-pacific
254 transport of ozone and its precursors to the U.S. West Coast (Hudman et al., 2004; Huang et al.,
255 2010; Lin et al., 2012b) and stratosphere-troposphere exchange of ozone to high altitude region
256 (Langford et al., 2009; Lin et al., 2012a).

257

258 **3.3. Ozone trends derived from CMAQ simulations**

259 We applied the same box-averaging technique to hourly surface ozone simulations
260 in CONUS and conducted the linear regression analysis to estimate the ozone trend at each
261 model grid (Fig. 8). Compared with ozone trends derived from AQS observations (Fig. 7), the
262 CMAQ model successfully captured the spatial pattern and magnitude of change in ozone
263 pollution. For instance, at 4 pm LT, CMAQ simulated up to 0.4 ppbv/yr decrease in surface
264 ozone in the eastern United States and south region of California state. However, CMAQ
265 simulated statistically insignificant trends (white color in Fig. 8c) at 4 pm LT in the Bay area,
266 Los Angeles, and Denver where AQS observations showed increasing trends (Fig. 7c). The
267 discrepancy occurred because our model used the static chemical lateral conditions (LBCs) that



268 did not include the change of trans-Pacific transport of air pollutants, which were known to
269 elevate the background ozone in the West Coast. Also CMAQ does not contain stratospheric
270 chemistry and hence cannot account the contribution of downward transport of stratospheric
271 ozone to the high altitude region.

272 Consistent with trends derived from AQS observations, CMAQ also simulated increasing
273 ozone trends in the early morning (8 am LT, Fig. 8a) and late afternoon (8 pm LT, Fig 8d),
274 especially in urban regions such as Los Angeles and Chicago. He et al. (2019) found ozone
275 increases from observations at four sites in the eastern United States and a possible cause
276 suggested by the reduced NO-O₃ titration through examining the trend in odd oxygen ($O_x = O_3 +$
277 NO_2). Due to known interferences from nitrogen compounds such as NO_x and organic nitrates to
278 standard NO₂ measurements employed by EPA (Fehsenfeld et al., 1987; Dunlea et al., 2007), the
279 analysis of O_x required research grade NO₂ analyzer (e.g., photolytic NO₂ conversion) which are
280 not available in current AQS network. Thus, our simulations provide a unique opportunity to
281 expand such study to the whole CONUS.

282 Trends in O_x concentrations simulated by CMAQ at 8 am, 12 pm, 4 pm, and 8 pm show a
283 consistent decreasing trend over the modeling domain, up to 0.5 ppbv/yr reductions in the eastern
284 United States (Fig. 9). The result confirms our hypothesis that the reduced NO-O₃ titration
285 elevated surface ozone concentrations in the early morning and late afternoon when the
286 photochemical production of ozone is low or not active. The current EPA ozone standard focuses
287 on peak ozone concentrations, i.e., MDA8 ozone which usually has maximum values at noon or
288 in the early afternoon, so the damage from additional ozone exposure from these elevated ozone
289 concentrations in the early morning and late afternoon is not considered under the current
290 environment policy. These increased ozone levels could offset the benefit from reduced peak



291 ozone in past decades, which needs further investigation to provide scientific evidence for future
292 policy decision.

293

294 **3.4 Change in photochemical regime**

295 With the continuous reduction of ozone precursor emissions, changes in the complex O₃-
296 NO_x-VOC chemistry are anticipated. We used the O₃/NO_y ratio as the indicator to study the
297 photochemical regime change in the U.S. surface ozone production. The threshold of 15
298 proposed by Zhang et al. (2009b) was adopted to identify the VOC-sensitive or NO_x-sensitive
299 regime, i.e., O₃/NO_y < 15 indicating the VOC-sensitive regime. For each local hour, we
300 calculated the probability when O₃/NO_y is lower than 15 in every month. Figure 10 shows the
301 probability of VOC-sensitive regime at 2 pm in July of 1995, 2005, and 2015. Most regions
302 dominated by the VOC-sensitive chemistry are urban or suburban where anthropogenic NO_x
303 emissions are relatively high as compared with anthropogenic and/or biogenic VOCs emissions,
304 such as the Los Angeles basin, the Northeast corridor (Washington D.C.-Baltimore-Philadelphia-
305 NYC), and the Chicago metropolitan area. Noting that these maps are created based on ozone
306 photochemical production simulated at the surface level, so the distributions are slightly different
307 from recent studies using satellite data (Duncan et al., 2010; Jin et al., 2017; Ring et al., 2018).

308 We calculated the mean probability of VOC-sensitivity (2 pm in July) in a 3 × 3 grid in
309 metropolitan areas of Baltimore, Los Angeles, and NYC from 1990 to 2015 (Fig. 11). CMAQ
310 simulations suggest the transition from VOC-sensitive regime to NO_x-sensitive regime in these
311 urban areas. There were interannual variabilities in the probability of VOC-sensitive
312 photochemistry in Baltimore (~50%) and NYC (~80%) in the 1990s and the early 2000s. After
313 the EPA 2003 NO_x SIP call, anthropogenic NO_x emissions decreased substantially leading to



314 reduced ozone pollution in the eastern United States (He et al., 2013), so the photochemical
315 production of surface ozone is expected to gradually become NO_x -sensitive. In 2015, ozone
316 photochemical production in Baltimore was dominated by NO_x emissions (only ~20%
317 probability of VOC-sensitive), while NYC had higher probability (>50%) of VOC-sensitive
318 chemistry. In Los Angeles, ozone chemistry slowly leaned to NO_x -sensitive, but until 2015 the
319 local ozone production was still controlled by VOCs emissions. In regions with VOC-sensitive
320 photochemistry in summer, reduction in NO_x emissions had a limited impact on the local rate of
321 ozone production until the photochemistry of ozone production became NO_x -sensitive. Our
322 analysis can partially explain the different responses of ozone pollution in major U.S. cities to
323 national air quality regulations during the past decades (Cooper et al., 2012) and can provide
324 some insights for future policy decision.

325

326 **4. Conclusions and Discussion**

327 EPA AQS observations in the United States from 1990 to 2015 were analyzed to study the
328 trend in surface ozone seasonal variations and diurnal cycles. We showed that the peak ozone
329 concentrations in the afternoon decreased significantly, especially in major non-attainment
330 regions, but the concentrations in the early morning and late afternoon increased slightly.
331 Regional climate-air quality model captured the long-term records of U.S. ozone pollution and
332 suggested that the increased ozone was caused by reduced $\text{NO}-\text{O}_3$ titration due to the continuous
333 reduction of NO_x emissions. Model simulations also showed changes in ozone photochemical
334 regime. The U.S. urban/suburban areas generally transited from the VOC-sensitive regime in the
335 early 1990s to more NO_x -sensitive regime recently. But ozone production in some cities such as
336 NYC and Los Angeles are still substantially impacted by VOC emissions. The current national



337 and regional regulations focus on the MDA8 ozone concentrations mainly determined by the
338 peak ozone in the afternoon. Our study revealed the elevated ozone concentrations in the early
339 morning and late afternoon which must be considered for their impacts on public health. While
340 NO_x emissions are currently the main target of national and regional control measures, our study
341 suggested that regulations on anthropogenic VOCs emissions could be important in certain
342 regions. This study can improve our understanding about the effectiveness of regulations in the
343 past decades and will provide scientific evidence for future policy decision.

344 Ozone production is highly non-linear, so accurate emissions are essential to simulate its
345 long-term variations. Due to limited resources, we scaled the anthropogenic emissions from a
346 baseline year (2014) to the 1990s using factors derived from the national trend data. This scaling
347 cannot accurately reflect the detailed regional-dependent regulations for individual state such as
348 the 2012 Health Air Act in Maryland (He et al., 2016b). Also, because the GFED data were only
349 available after 1997, the contribution of wildfire emissions to ozone pollution was not included
350 in model simulations between 1990 to 1996. Thus, we anticipated some uncertainties in ozone
351 simulations in the early 1990s. Our model also has limitations to reproduce ozone records in high
352 altitude regions such as Denver because of lacking the stratospheric chemistry in CMAQ and
353 missing the effect of stratosphere-troposphere exchange to surface ozone. Lastly, due to limited
354 resources, our experiments used static chemical LBCs for CMAQ, which excluded the long-
355 range transport of air pollutants into the United States. For some West Coast regions such as the
356 state of California, the trans-Pacific transport had been enhanced in the past decades and could
357 play a more important role in determining the local air quality. To accurately evaluate the
358 contribution from trans-boundary emission, dynamic LBCs from a global chemical transport
359 model is needed in the future study.



360 **Author contribution**

361 H.H., X.L., and Z.T. designed the experiment; H.H. and C.S. developed the CWRP-CMAQ
362 system and performed the CWRP modeling; Z.T. and D.T. prepared the emission data; H.H.
363 conducted the CMAQ simulations; H.H., Z.T., and C.S. analyzed the data; H.H. prepared the
364 manuscript with contributions from all co-authors.

365

366 **Acknowledgments**

367 This work was supported by the U.S. Environmental Protection Agency under Assistance
368 Agreement No. RD-83587601. It has not been formally reviewed by EPA. The views expressed
369 in this document are solely those of the authors and do not necessarily reflect those of the
370 funding Agency. EPA does not endorse any products or commercial services mentioned in this
371 publication. We thank the support of University of Illinois at Urbana-Champaign
372 (UIUC)/USEPA award 20110150701. We thank the National Center for Supercomputing
373 Applications (NCSA) and the National Center for Atmospheric Research (NCAR) Computation
374 and Information System Laboratory for supercomputing support. We thank Dr. Plessel Todd for
375 the help on the RSIG software (<https://www.epa.gov/rsig>).

376

377 **References**

- 378 Adams, R. M., Glycer, J. D., Johnson, S. L., and McCarl, B. A.: A reassessment of the economic-effects of ozone on
379 United-States agriculture, *Japca-the Journal of the Air & Waste Management Association*, 39, 960-968,
380 1989.
- 381 Anderson, H. R.: Air pollution and mortality: A history, *Atmospheric Environment*, 43, 142-152,
382 10.1016/j.atmosenv.2008.09.026, 2009.
- 383 Appel, K. W., Napelenok, S. L., Hogrefe, C., Foley, K. M., Pouliot, G., Murphy, B. N., Luecken, D. J., and Heath,
384 N.: Evaluation of the Community Multiscale Air Quality (CMAQ) Model Version 5.2, 2016 CMAS
385 Conference, Chapel Hill, NC., 2016.
- 386 Ashmore, M. R.: Assessing the future global impacts of ozone on vegetation, *Plant Cell Environ.*, 28, 949-964,
387 10.1111/j.1365-3040.2005.01341.x, 2005.
- 388 Briggs, G. A.: Chimney plumes in neutral and stable surroundings**Shwartz and Tulin, *Atmospheric Environment*,
389 19-35 (1971), *Atmospheric Environment* (1967), 6, 507-510, [https://doi.org/10.1016/0004-6981\(72\)90120-](https://doi.org/10.1016/0004-6981(72)90120-5)
390 5, 1972.
- 391 Chen, L. G., Liang, X. Z., DeWitt, D., Samel, A. N., and Wang, J. X. L.: Simulation of seasonal US precipitation and



- 392 temperature by the nested CWRP-ECHAM system, *Climate Dynamics*, 46, 879-896, 10.1007/s00382-015-
393 2619-9, 2016.
- 394 Chou, M.-D., Suarez, M. J., Liang, X.-Z., Yan, M. M.-H., and Cote, C.: A thermal infrared radiation
395 parameterization for atmospheric studies, 2001.
- 396 Cooper, O., Parrish, D., Ziemke, J., Balashov, N., Cupeiro, M., Galbally, I., Gilge, S., Horowitz, L., Jensen, N., and
397 Lamarque, J.-F.: Global distribution and trends of tropospheric ozone: An observation-based review,
398 *Elementa: Science of the Anthropocene*, 2, 000029, 2014.
- 399 Cooper, O. R., Gao, R. S., Tarasick, D., Leblanc, T., and Sweeney, C.: Long-term ozone trends at rural ozone
400 monitoring sites across the United States, 1990-2010, *Journal of Geophysical Research-Atmospheres*, 117,
401 D22307, 10.1029/2012jd018261, 2012.
- 402 Crutzen, P. J.: Photochemical reactions initiated by and influencing ozone in unpolluted tropospheric air, *Tellus*, 26,
403 47-57, 1974.
- 404 Dee, D. P., Uppala, S. M., Simmons, A. J., Berrisford, P., Poli, P., Kobayashi, S., Andrae, U., Balmaseda, M. A.,
405 Balsamo, G., Bauer, P., Bechtold, P., Beljaars, A. C. M., van de Berg, L., Bidlot, J., Bormann, N., Delsol,
406 C., Dragani, R., Fuentes, M., Geer, A. J., Haimberger, L., Healy, S. B., Hersbach, H., Hólm, E. V., Isaksen,
407 L., Kållberg, P., Köhler, M., Matricardi, M., McNally, A. P., Monge-Sanz, B. M., Morcrette, J. J., Park, B.
408 K., Peubey, C., de Rosnay, P., Tavolato, C., Thépaut, J. N., and Vitart, F.: The ERA-Interim reanalysis:
409 configuration and performance of the data assimilation system, *Q. J. R. Meteorol. Soc.*, 137, 553-597,
410 10.1002/qj.828, 2011.
- 411 Dodge, M.: *Chemistry of Oxidant Formation: Implications for Designing Effective Control Strategies U.S.*
412 *Environmental Protection Agency, Washington, D.C. EPA/600/D-87/114 (NTIS PB87179990)*, 1987.
- 413 Duncan, B. N., Yoshida, Y., Olson, J. R., Sillman, S., Martin, R. V., Lamsal, L., Hu, Y. T., Pickering, K. E., Retscher,
414 C., Allen, D. J., and Crawford, J. H.: Application of OMI observations to a space-based indicator of NO_x
415 and VOC controls on surface ozone formation, *Atmospheric Environment*, 44, 2213-2223,
416 10.1016/j.atmosenv.2010.03.010, 2010.
- 417 Dunlea, E. J., Herndon, S. C., Nelson, D. D., Volkamer, R. M., San Martini, F., Sheehy, P. M., Zahniser, M. S.,
418 Shorter, J. H., Wormhoudt, J. C., Lamb, B. K., Allwine, E. J., Gaffney, J. S., Marley, N. A., Grutter, M.,
419 Marquez, C., Blanco, S., Cardenas, B., Retama, A., Villegas, C. R. R., Kolb, C. E., Molina, L. T., and
420 Molina, M. J.: Evaluation of nitrogen dioxide chemiluminescence monitors in a polluted urban
421 environment, *Atmospheric Chemistry and Physics*, 7, 2691-2704, 2007.
- 422 EPA: CMAQ (Version 5.2) Scientific Document, Zenodo. <http://doi.org/10.5281/zenodo.1167892>, 2017.
- 423 EPA, U. S.: Air quality criteria for ozone and related photochemical oxidants, *Environ. Prot. Agency*, , Research
424 Triangle Park, N.C., 2006.
- 425 Fehsenfeld, F. C., Dickerson, R. R., Hubler, G., Luke, W. T., Nunnermacker, L. J., Williams, E. J., Roberts, J. M.,
426 Calvert, J. G., Curran, C. M., Delany, A. C., Eubank, C. S., Fahey, D. W., Fried, A., Gandrud, B. W.,
427 Langford, A. O., Murphy, P. C., Norton, R. B., Pickering, K. E., and Ridley, B. A.: A ground-based
428 intercomparison of NO, NO_x, and NO_y measurement techniques, *Journal of Geophysical Research-*
429 *Atmospheres*, 92, 14710-14722, 1987.
- 430 Finlayson-Pitts, B. J., and Pitts, J. N.: *Chemistry of the Upper and Lower Atmosphere*, 1st ed., Academic Press, UK,
431 1999.
- 432 Fiore, A., Jacob, D. J., Liu, H., Yantosca, R. M., Fairlie, T. D., and Li, Q.: Variability in surface ozone background
433 over the United States: Implications for air quality policy, *Journal of Geophysical Research: Atmospheres*,
434 108, 10.1029/2003jd003855, 2003.
- 435 Fiore, A. M., Jacob, D. J., Bey, I., Yantosca, R. M., Field, B. D., Fusco, A. C., and Wilkinson, J. G.: Background
436 ozone over the United States in summer: Origin, trend, and contribution to pollution episodes, *Journal of*
437 *Geophysical Research: Atmospheres*, 107, ACH 11-11-ACH 11-25, 10.1029/2001jd000982, 2002.
- 438 Fishman, J., Ramanathan, V., Crutzen, P. J., and Liu, S. C.: Tropospheric ozone and climate, *Nature*, 282, 818-820,
439 10.1038/282818a0, 1979.
- 440 He, H., Stehr, J. W., Hains, J. C., Krask, D. J., Doddridge, B. G., Vinnikov, K. Y., Canty, T. P., Hosley, K. M.,
441 Salawitch, R. J., Worden, H. M., and Dickerson, R. R.: Trends in emissions and concentrations of air
442 pollutants in the lower troposphere in the Baltimore/Washington airshed from 1997 to 2011, *Atmospheric*
443 *Chemistry and Physics*, 13, 7859-7874, 10.5194/acp-13-7859-2013, 2013.
- 444 He, H., Liang, X.-Z., Lei, H., and Wuebbles, D. J.: Future U.S. ozone projections dependence on regional emissions,
445 climate change, long-range transport and differences in modeling design, *Atmospheric Environment*, 128,
446 124-133, <https://doi.org/10.1016/j.atmosenv.2015.12.064>, 2016a.
- 447 He, H., Vinnikov, K. Y., Li, C., Krotkov, N. A., Jongeward, A. R., Li, Z. Q., Stehr, J. W., Hains, J. C., and Dickerson,



- 448 R. R.: Response of SO₂ and particulate air pollution to local and regional emission controls: A case study in
449 Maryland, *Earth Future*, 4, 94-109, 10.1002/2015ef000330, 2016b.
- 450 He, H., Liang, X. Z., and Wuebbles, D. J.: Effects of emissions change, climate change and long-range transport on
451 regional modeling of future US particulate matter pollution and speciation, *Atmospheric Environment*, 179,
452 166-176, 10.1016/j.atmosenv.2018.02.020, 2018.
- 453 He, H., Vinnikov, K. Y., Krotkov, N. A., Edgerton, E. S., Schwab, J. J., and Dickerson, R. R.: Chemical climatology
454 of atmospheric pollutants in the eastern United States: Seasonal/diurnal cycles and contrast under
455 clear/cloudy conditions for remote sensing, *Atmospheric Environment*, 206, 85-107,
456 <https://doi.org/10.1016/j.atmosenv.2019.03.003>, 2019.
- 457 Hogrefe, C., Hao, W., Zalewsky, E. E., Ku, J. Y., Lynn, B., Rosenzweig, C., Schultz, M. G., Rast, S., Newchurch, M.
458 J., Wang, L., Kinney, P. L., and Sistla, G.: An analysis of long-term regional-scale simulations over
459 the Northeastern United States: variability and trends, *Atmospheric Chemistry and Physics*, 11, 567-582,
460 10.5194/acp-11-567-2011, 2011.
- 461 Holton, J. R., Haynes, P. H., McIntyre, M. E., Douglass, A. R., Rood, R. B., and Pfister, L.: Stratosphere-troposphere
462 exchange, *Reviews of Geophysics*, 33, 403-439, 10.1029/95rg02097, 1995.
- 463 Holtslag, A. A. M., and Boville, B. A.: Local Versus Nonlocal Boundary-Layer Diffusion in a Global Climate
464 Model, *Journal of Climate*, 6, 1825-1842, 10.1175/1520-0442(1993)006<1825:lvnbl>2.0.co;2, 1993.
- 465 Houyoux, M. R., Vukovich, J. M., Coats Jr., C. J., Wheeler, N. J. M., and Kasibhatla, P. S.: Emission inventory
466 development and processing for the Seasonal Model for Regional Air Quality (SMRAQ) project, *Journal of
467 Geophysical Research: Atmospheres*, 105, 9079-9090, 10.1029/1999jd900975, 2000.
- 468 Huang, H. C., Liang, X. Z., Kunkel, K. E., Caughey, M., and Williams, A.: Seasonal simulation of tropospheric
469 ozone over the midwestern and northeastern United States: An application of a coupled regional climate
470 and air quality modeling system, *J. Appl. Meteorol. Climatol.*, 46, 945-960, 10.1175/jam2521.1, 2007.
- 471 Huang, M., Carmichael, G., Adhikary, B., Spak, S., Kulkarni, S., Cheng, Y., Wei, C., Tang, Y., Parrish, D., and
472 Oltmans, S.: Impacts of transported background ozone on California air quality during the ARCTAS-CARB
473 period—a multi-scale modeling study, *Atmospheric Chemistry and Physics*, 10, 6947-6968, 2010.
- 474 Hudman, R., Jacob, D. J., Cooper, O., Evans, M., Heald, C., Park, R., Fehsenfeld, F., Flocke, F., Holloway, J., and
475 Hübler, G.: Ozone production in transpacific Asian pollution plumes and implications for ozone air quality
476 in California, *Journal of Geophysical Research: Atmospheres*, 109, 2004.
- 477 IPCC: Climate Change 2013: The Physical Science Basis., Contribution of Working Group I to the Fifth Assessment
478 Report (AR5) of the Intergovernmental Panel on Climate Change, 1535 pp.,
479 doi:10.1017/CBO9781107415324, 2013.
- 480 Jacob, D. J.: Heterogeneous chemistry and tropospheric ozone, *Atmospheric Environment*, 34, 2131-2159,
481 10.1016/s1352-2310(99)00462-8, 2000.
- 482 Jaffe, D., and Ray, J.: Increase in surface ozone at rural sites in the western US, *Atmospheric Environment*, 41,
483 5452-5463, 10.1016/j.atmosenv.2007.02.34, 2007.
- 484 Jerrett, M., Burnett, R. T., Pope, C. A., Ito, K., Thurston, G., Krewski, D., Shi, Y., Calle, E., and Thun, M.: Long-
485 Term Ozone Exposure and Mortality, *N. Engl. J. Med.*, 360, 1085-1095, 10.1056/NEJMoa0803894, 2009.
- 486 Jin, X., Fiore, A. M., Murray, L. T., Valin, L. C., Lamsal, L. N., Duncan, B., Folkert Boersma, K., De Smedt, I.,
487 Abad, G. G., Chance, K., and Tonnesen, G. S.: Evaluating a Space-Based Indicator of Surface Ozone-NO_x-
488 VOC Sensitivity Over Midlatitude Source Regions and Application to Decadal Trends, *Journal of
489 Geophysical Research: Atmospheres*, 122, 4039-4104, doi:10.1002/2017JD026720, 2017.
- 490 Kleinman, L. I.: Low and high NO_x tropospheric photochemistry, *Journal of Geophysical Research-Atmospheres*,
491 99, 16831-16838, 10.1029/94jd01028, 1994.
- 492 Langford, A., Aikin, K., Eubank, C., and Williams, E.: Stratospheric contribution to high surface ozone in Colorado
493 during springtime, *Geophysical Research Letters*, 36, 2009.
- 494 Lefohn, A. S., Shadwick, D., and Oltmans, S. J.: Characterizing long-term changes in surface ozone levels in the
495 United States (1980-2005), *Atmospheric Environment*, 42, 8252-8262, 10.1016/j.atmosenv.2008.07.060,
496 2008.
- 497 Lefohn, A. S., Shadwick, D., and Oltmans, S. J.: Characterizing changes in surface ozone levels in metropolitan and
498 rural areas in the United States for 1980-2008 and 1994-2008, *Atmospheric Environment*, 44, 5199-5210,
499 10.1016/j.atmosenv.2010.08.049, 2010.
- 500 Lefohn, A. S., Emery, C., Shadwick, D., Wernli, H., Jung, J., and Oltmans, S. J.: Estimates of background surface
501 ozone concentrations in the United States based on model-derived source apportionment, *Atmospheric
502 Environment*, 84, 275-288, <https://doi.org/10.1016/j.atmosenv.2013.11.033>, 2014.
- 503 Levy, H., Mahlman, J. D., Moxim, W. J., and Liu, S. C.: Tropospheric ozone - the role of transport, *Journal of*



- 504 Geophysical Research-Atmospheres, 90, 3753-3772, 10.1029/JD090iD02p03753, 1985.
- 505 Liang, X.-Z., Xu, M., Yuan, X., Ling, T., Choi, H. I., Zhang, F., Chen, L., Liu, S., Su, S., Qiao, F., He, Y., Wang, J.
- 506 X. L., Kunkel, K. E., Gao, W., Joseph, E., Morris, V., Yu, T.-W., Dudhia, J., and Michalakes, J.: Regional
- 507 Climate-Weather Research and Forecasting Model, Bulletin of the American Meteorological Society, 93,
- 508 1363-1387, 10.1175/bams-d-11-00180.1, 2012.
- 509 Liang, X.-Z., Sun, C., Zheng, X., Dai, Y., Xu, M., Choi, H. I., Ling, T., Qiao, F., Kong, X., Bi, X., Song, L., and
- 510 Wang, F.: CWRf performance at downscaling China climate characteristics, Climate Dynamics, 52, 2159-
- 511 2184, 10.1007/s00382-018-4257-5, 2019a.
- 512 Liang, X.-Z., Sun, C., Zheng, X., Dai, Y., Xu, M., Choi, H. I., Ling, T., Qiao, F., Kong, X., Bi, X., Song, L., and
- 513 Wang, F.: CWRf performance at downscaling China climate characteristics, Climate Dynamics,
- 514 10.1007/s00382-018-4257-5, 2019b.
- 515 Lin, M., Fiore, A. M., Cooper, O. R., Horowitz, L. W., Langford, A. O., Levy, H., Johnson, B. J., Naik, V., Oltmans,
- 516 S. J., and Senff, C. J.: Springtime high surface ozone events over the western United States: Quantifying
- 517 the role of stratospheric intrusions, Journal of Geophysical Research: Atmospheres, 117, 2012a.
- 518 Lin, M., Fiore, A. M., Horowitz, L. W., Cooper, O. R., Naik, V., Holloway, J., Johnson, B. J., Middlebrook, A. M.,
- 519 Oltmans, S. J., and Pollack, I. B.: Transport of Asian ozone pollution into surface air over the western
- 520 United States in spring, Journal of Geophysical Research: Atmospheres, 117, 2012b.
- 521 Liu, S., Wang, J. X. L., Liang, X.-Z., and Morris, V.: A hybrid approach to improving the skills of seasonal climate
- 522 outlook at the regional scale, Climate Dynamics, 46, 483-494, 10.1007/s00382-015-2594-1, 2016a.
- 523 Liu, S. Y., Wang, J., Liang, X. Z., and Morris, V.: A hybrid approach to improving the skills of seasonal climate
- 524 outlook at the regional scale, Climate Dynamics, 46, 483-494, 10.1007/s00382-015-2594-1, 2016b.
- 525 Logan, J. A., Prather, M. J., Wofsy, S. C., and McElroy, M. B.: Tropospheric chemistry - a global perspective,
- 526 Journal of Geophysical Research-Oceans and Atmospheres, 86, 7210-7254, 10.1029/JC086iC08p07210,
- 527 1981.
- 528 Oltmans, S. J., Lefohn, A. S., Harris, J. M., Galbally, I., Scheel, H. E., Bodeker, G., Brunke, E., Claude, H., Tarasick,
- 529 D., Johnson, B. J., Simmonds, P., Shadwick, D., Anlauf, K., Hayden, K., Schmidlin, F., Fujimoto, T., Akagi,
- 530 K., Meyer, C., Nichol, S., Davies, J., Redondas, A., and Cuevas, E.: Long-term changes in tropospheric
- 531 ozone, Atmospheric Environment, 40, 3156-3173, 10.1016/j.atmosenv.2006.01.029, 2006.
- 532 Peng, Y. P., Chen, K. S., Wang, H. K., and Lai, C. H.: In Situ Measurements of Hydrogen Peroxide, Nitric Acid and
- 533 Reactive Nitrogen to Assess the Ozone Sensitivity in Pingtung County, Taiwan, Aerosol and Air Quality
- 534 Research, 11, 59-69, 10.4209/aaqr.2010.10.0091, 2011.
- 535 Pour-Biazar, A., Khan, M., Wang, L. H., Park, Y. H., Newchurch, M., McNider, R. T., Liu, X., Byun, D. W., and
- 536 Cameron, R.: Utilization of satellite observation of ozone and aerosols in providing initial and boundary
- 537 condition for regional air quality studies, Journal of Geophysical Research-Atmospheres, 116, D18309,
- 538 10.1029/2010jd015200, 2011.
- 539 Qiao, F., and Liang, X.-Z.: Effects of cumulus parameterization closures on simulations of summer precipitation
- 540 over the continental United States, Climate Dynamics, 49, 225-247, 10.1007/s00382-016-3338-6, 2017.
- 541 Qiao, F. X., and Liang, X. Z.: Effects of cumulus parameterizations on predictions of summer flood in the Central
- 542 United States, Climate Dynamics, 45, 727-744, 10.1007/s00382-014-2301-7, 2015.
- 543 Qiao, F. X., and Liang, X. Z.: Effects of cumulus parameterization closures on simulations of summer precipitation
- 544 over the United States coastal oceans, J. Adv. Model. Earth Syst., 8, 764-785, 10.1002/2015ms000621,
- 545 2016.
- 546 Ramanathan, V., and Dickinson, R. E.: Role of stratospheric ozone in the zonal and seasonal radiative energy-
- 547 balance of the Earth-troposphere system, Journal of the Atmospheric Sciences, 36, 1084-1104, 1979.
- 548 Randerson, J. T., Van Der Werf, G. R., Giglio, L., Collatz, G. J., and Kasibhatla, P. S.: Global Fire Emissions
- 549 Database, Version 4.1 (GFEDv4). ORNL Distributed Active Archive Center, 2017.
- 550 Ring, A. M., Canty, T. P., Anderson, D. C., Vinciguerra, T. P., He, H., Goldberg, D. L., Ehrman, S. H., Dickerson, R.
- 551 R., and Salawitch, R. J.: Evaluating commercial marine emissions and their role in air quality policy using
- 552 observations and the CMAQ model, Atmospheric Environment, 173, 96-107,
- 553 <https://doi.org/10.1016/j.atmosenv.2017.10.037>, 2018.
- 554 Seinfeld, J. H., and Pandis, S. N.: Atmospheric Chemistry and Physics: From Air Pollution to Climate Change, 2nd
- 555 ed., John Wiley & Sons, Inc., 2006.
- 556 Seinfeld, J. H. e. a.: Rethinking the Ozone Problem in Urban and Regional Air Pollution, National Academics Press,
- 557 Washington, DC, 1991.
- 558 Shon, Z.-H., Lee, G., Song, S.-K., Lee, M., Han, J., and Lee, D.: Characteristics of reactive nitrogen compounds and
- 559 other relevant trace gases in the atmosphere at urban and rural areas of Korea during May-June, 2004,



- 560 Journal of Atmospheric Chemistry, 58, 203-218, 10.1007/s10874-007-9088-4, 2007.
- 561 Sillman, S.: The use of NO_y, H₂O₂, and HNO₃ as indicators for ozone-NO_x-hydrocarbon sensitivity in urban
562 locations, *Journal of Geophysical Research-Atmospheres*, 100, 14175-14188, 10.1029/94jd02953, 1995.
- 563 Sillman, S., He, D., Cardelino, C., and Imhoff, R. E.: The Use of Photochemical Indicators to Evaluate Ozone-NO_x-
564 Hydrocarbon Sensitivity: Case Studies from Atlanta, New York, and Los Angeles, *J. Air Waste Manage.*
565 *Assoc.*, 47, 1030-1040, 10.1080/10962247.1997.11877500, 1997.
- 566 Sillman, S.: The relation between ozone, NO_x and hydrocarbons in urban and polluted rural environments,
567 *Atmospheric Environment*, 33, 1821-1845, 10.1016/s1352-2310(98)00345-8, 1999.
- 568 Sillman, S., and He, D.: Some theoretical results concerning O₃-NO_x-VOC chemistry and NO_x-VOC indicators,
569 *Journal of Geophysical Research: Atmospheres*, 107, ACH 26-21-ACH 26-15, 10.1029/2001jd001123,
570 2002.
- 571 Stevenson, D. S., Dentener, F. J., Schultz, M. G., Ellingsen, K., van Noije, T. P. C., Wild, O., Zeng, G., Amann, M.,
572 Atherton, C. S., Bell, N., Bergmann, D. J., Bey, I., Butler, T., Cofala, J., Collins, W. J., Derwent, R. G.,
573 Doherty, R. M., Drevet, J., Eskes, H. J., Fiore, A. M., Gauss, M., Hauglustaine, D. A., Horowitz, L. W.,
574 Isaksen, I. S. A., Krol, M. C., Lamarque, J. F., Lawrence, M. G., Montanaro, V., Müller, J. F., Pitari, G.,
575 Prather, M. J., Pyle, J. A., Rast, S., Rodriguez, J. M., Sanderson, M. G., Savage, N. H., Shindell, D. T.,
576 Strahan, S. E., Sudo, K., and Szopa, S.: Multimodel ensemble simulations of present-day and near-future
577 tropospheric ozone, *Journal of Geophysical Research-Atmospheres*, 111, D08301, 10.1029/2005jd006338,
578 2006.
- 579 Sun, C., and Liang, X. Z.: Improving U.S. extreme precipitation simulation: Dependence on cumulus
580 parameterization and underlying mechanism, *Journal of Climate*, under review, 2019a.
- 581 Sun, C., and Liang, X. Z.: Improving U.S. extreme precipitation simulation: Sensitivity to physics parameterizations,
582 *Journal of Climate*, under review, 2019b.
- 583 Tagaris, E., Manomaiphiboon, K., Liao, K.-J., Leung, L. R., Woo, J.-H., He, S., Amar, P., and Russell, A. G.:
584 Impacts of global climate change and emissions on regional ozone and fine particulate matter
585 concentrations over the United States, *Journal of Geophysical Research: Atmospheres*, 112,
586 doi:10.1029/2006JD008262, 2007.
- 587 Tang, Y., Lee, P., Tsidulko, M., Huang, H.-C., McQueen, J. T., DiMego, G. J., Emmons, L. K., Pierce, R. B.,
588 Thompson, A. M., Lin, H.-M., Kang, D., Tong, D., Yu, S., Mathur, R., Pleim, J. E., Otte, T. L., Pouliot, G.,
589 Young, J. O., Schere, K. L., Davidson, P. M., and Stajner, I.: The impact of chemical lateral boundary
590 conditions on CMAQ predictions of tropospheric ozone over the continental United States, *Environmental*
591 *Fluid Mechanics*, 9, 43-58, 10.1007/s10652-008-9092-5, 2009.
- 592 Tao, W.-K., Simpson, J., and McCumber, M.: An Ice-Water Saturation Adjustment, *Mon. Weather Rev.*, 117, 231-
593 235, 10.1175/1520-0493(1989)117<0231:aiwsa>2.0.co;2, 1989.
- 594 Tong, D., Pan, L., Chen, W., Lamsal, L., Lee, P., Tang, Y., Kim, H., Kondragunta, S., and Stajner, I.: Impact of the
595 2008 Global Recession on air quality over the United States: Implications for surface ozone levels from
596 changes in NO_x emissions, *Geophysical Research Letters*, 43, 9280-9288, 10.1002/2016gl069885, 2016.
- 597 Tong, D. Q., Lamsal, L., Pan, L., Ding, C., Kim, H., Lee, P., Chai, T. F., Pickering, K. E., and Stajner, I.: Long-term
598 NO_x trends over large cities in the United States during the great recession: Comparison of satellite
599 retrievals, ground observations, and emission inventories, *Atmospheric Environment*, 107, 70-84,
600 10.1016/j.atmosenv.2015.01.035, 2015.
- 601 Tonnesen, G. S., and Dennis, R. L.: Analysis of radical propagation efficiency to assess ozone sensitivity to
602 hydrocarbons and NO_x : 1. Local indicators of instantaneous odd oxygen production sensitivity, *Journal of*
603 *Geophysical Research: Atmospheres*, 105, 9213-9225, 10.1029/1999jd900371, 2000a.
- 604 Tonnesen, G. S., and Dennis, R. L.: Analysis of radical propagation efficiency to assess ozone sensitivity to
605 hydrocarbons and NO_x : 2. Long-lived species as indicators of ozone concentration sensitivity, *Journal of*
606 *Geophysical Research: Atmospheres*, 105, 9227-9241, 10.1029/1999jd900372, 2000b.
- 607 van der Werf, G. R., Randerson, J. T., Giglio, L., van Leeuwen, T. T., Chen, Y., Rogers, B. M., Mu, M. Q., van
608 Marle, M. J. E., Morton, D. C., Collatz, G. J., Yokelson, R. J., and Kasibhatla, P. S.: Global fire emissions
609 estimates during 1997-2016, *Earth Syst. Sci. Data*, 9, 697-720, 10.5194/essd-9-697-2017, 2017.
- 610 Wang, H., Jacob, D. J., Le Sager, P., Streets, D. G., Park, R. J., Gilliland, A. B., and van Donkelaar, A.: Surface
611 ozone background in the United States: Canadian and Mexican pollution influences, *Atmospheric*
612 *Environment*, 43, 1310-1319, <https://doi.org/10.1016/j.atmosenv.2008.11.036>, 2009.
- 613 WHO: Health aspects of air pollution with particulate matter, ozone and nitrogen dioxide, *World Health*
614 *Organisation*, Bonn., 2003.
- 615 Xie, Y., Elleman, R., Jobson, T., and Lamb, B.: Evaluation of O₃-NO_x-VOC sensitivities predicted with the CMAQ



- 616 photochemical model using Pacific Northwest 2001 field observations, *Journal of Geophysical Research:*
617 *Atmospheres*, 116, 10.1029/2011jd015801, 2011.
- 618 Xu, K.-M., and Randall, D. A.: A Semiempirical Cloudiness Parameterization for Use in Climate Models, *Journal of*
619 *the Atmospheric Sciences*, 53, 3084-3102, 10.1175/1520-0469(1996)053<3084:ascpfu>2.0.co;2, 1996.
- 620 Yarwood, G. S., Whitten, G. Z., Jung, J., Heo, G., and Allen, D.: Development, Evaluation and Testing of Version 6
621 of the Carbon Bond Chemical Mechanism (CB6),
622 [https://www.tceq.texas.gov/assets/public/implementation/air/am/contracts/reports/pm/5820784005FY1026-](https://www.tceq.texas.gov/assets/public/implementation/air/am/contracts/reports/pm/5820784005FY1026-20100922-environ-cb6.pdf)
623 [20100922-environ-cb6.pdf](https://www.tceq.texas.gov/assets/public/implementation/air/am/contracts/reports/pm/5820784005FY1026-20100922-environ-cb6.pdf), 2010.
- 624 Yuan, X., and Liang, X. Z.: Improving cold season precipitation prediction by the nested CWRP-CFS system,
625 *Geophysical Research Letters*, 38, L02706, 10.1029/2010gl046104, 2011.
- 626 Zhang, Y., Vijayaraghavan, K., Wen, X. Y., Snell, H. E., and Jacobson, M. Z.: Probing into regional ozone and
627 particulate matter pollution in the United States: 1. A 1 year CMAQ simulation and evaluation using
628 surface and satellite data, *Journal of Geophysical Research-Atmospheres*, 114, 10.1029/2009jd011898,
629 2009a.
- 630 Zhang, Y., Wen, X. Y., Wang, K., Vijayaraghavan, K., and Jacobson, M. Z.: Probing into regional O₃ and particulate
631 matter pollution in the United States: 2. An examination of formation mechanisms through a process
632 analysis technique and sensitivity study, *Journal of Geophysical Research-Atmospheres*, 114,
633 10.1029/2009jd011900, 2009b.
- 634 Zhu, J. H., and Liang, X. Z.: Impacts of the Bermuda High on Regional Climate and Ozone over the United States,
635 *Journal of Climate*, 26, 1018-1032, 10.1175/jcli-d-12-00168.1, 2013.
- 636
637



638 **Tables and Figures**

639

640 **Table 1.** Summary of multiyear mean average of daily CO, NO_x, and NMVOCs emissions in the
 641 CONUS and five subdomains. (Unit: mol/km² per second) Please note that our California and
 642 Texas subdomains include more area than the states of California and Texas.
 643

CONUS				Southeast		
Year	CO	NO _x	NMVOCs	CO	NO _x	NMVOCs
1990-1994	32.9	1.24	0.94	47.2	1.43	1.03
1995-1999	26.2	1.18	0.76	37.4	1.36	0.85
2000-2004	18.9	1.26	0.69	26.4	1.46	0.72
2005-2009	12.3	0.94	0.60	16.9	1.07	0.59
2010-2015	8.0	0.60	0.46	11.0	0.66	0.45
California				Northeast		
1990-1994	18.3	1.22	0.57	110.3	3.29	2.12
1995-1999	14.6	1.16	0.46	87.2	3.16	1.68
2000-2004	10.6	1.23	0.40	62.1	3.41	1.43
2005-2009	7.1	0.91	0.35	40.3	2.56	1.25
2010-2015	4.6	0.56	0.26	25.9	1.62	0.93
Texas				Midwest		
1990-1994	22.6	1.21	1.26	58.2	1.88	1.41
1995-1999	18.1	1.15	1.03	46.3	1.80	1.14
2000-2004	13.0	1.20	1.01	33.4	1.92	0.98
2005-2009	8.4	0.91	0.92	22.0	1.44	0.85
2010-2015	5.5	0.60	0.73	14.3	0.91	0.63

644



645 **Table 2.** Summary about the comparison of JJA MDA8 ozone concentrations from AQS
 646 observations and CMAQ simulations during 2000-2015 in the CONUS and subdomains. Slope
 647 and Correlation (Corr. R) are calculated for each year based on linear regression analysis. Please
 648 note that our California and Texas subdomains include more area than the states of California
 649 and Texas.
 650

Year	Slope	Corr. R	NMB	RMSE	Year	Slope	Corr. R	NMB	RMSE
CONUS									
2000	0.73	0.37	-6.9	10.5	2008	0.70	0.54	-5.4	8.4
2001	0.80	0.61	-7.7	8.7	2009	0.78	0.35	-1.6	8.5
2002	0.71	0.63	-8.6	9.2	2010	0.75	0.51	-6.2	8.4
2003	0.81	0.60	-4.3	8.4	2011	0.77	0.42	-7.1	9.2
2004	0.85	0.39	1.3	8.9	2012	0.67	0.60	-10.7	9.3
2005	0.87	0.54	-7.3	8.8	2013	0.70	0.50	-1.8	7.9
2006	0.77	0.48	-7.6	9.1	2014	0.72	0.44	-3.0	7.6
2007	0.70	0.60	-6.1	8.0	2015	0.73	0.41	-4.2	7.7
California									
2000	0.70	0.67	-19.3	15.2	2008	0.63	0.53	-18.0	14.8
2001	0.72	0.63	-18.1	14.8	2009	0.67	0.61	-19.0	13.5
2002	0.80	0.55	-15.5	14.4	2010	0.62	0.55	-19.0	14.1
2003	0.80	0.55	-20.1	16.2	2011	0.68	0.57	-17.0	13.3
2004	0.78	0.51	-19.2	16.1	2012	0.64	0.63	-21.4	14.9
2005	0.78	0.54	-19.0	15.3	2013	0.64	0.60	-17.9	13.5
2006	0.80	0.61	-20.5	15.6	2014	0.69	0.56	-21.9	14.8
2007	0.69	0.65	-16.0	12.9	2015	0.72	0.61	-22.3	14.2
Texas									
2000	0.60	0.77	-20.4	11.8	2008	0.62	0.74	-10.5	6.6
2001	0.58	0.62	-19.6	11.5	2009	0.73	0.78	-17.1	8.7
2002	0.70	0.72	-10.4	6.6	2010	0.65	0.77	-9.4	5.3
2003	0.64	0.78	-8.8	6.5	2011	0.52	0.83	-22.7	12.1
2004	0.97	0.55	-7.2	5.8	2012	0.53	0.86	-17.8	9.4
2005	0.70	0.78	-21.5	11.4	2013	0.53	0.74	-11.6	6.9
2006	0.66	0.83	-20.5	11.3	2014	0.66	0.72	-5.0	4.7
2007	0.77	0.84	-4.0	3.9	2015	0.76	0.61	-10.1	5.8
Southeast									
2000	0.61	0.41	-20.5	13.3	2008	0.52	0.77	-13.4	8.3
2001	0.64	0.70	-7.7	6.2	2009	0.88	0.52	-2.7	4.2

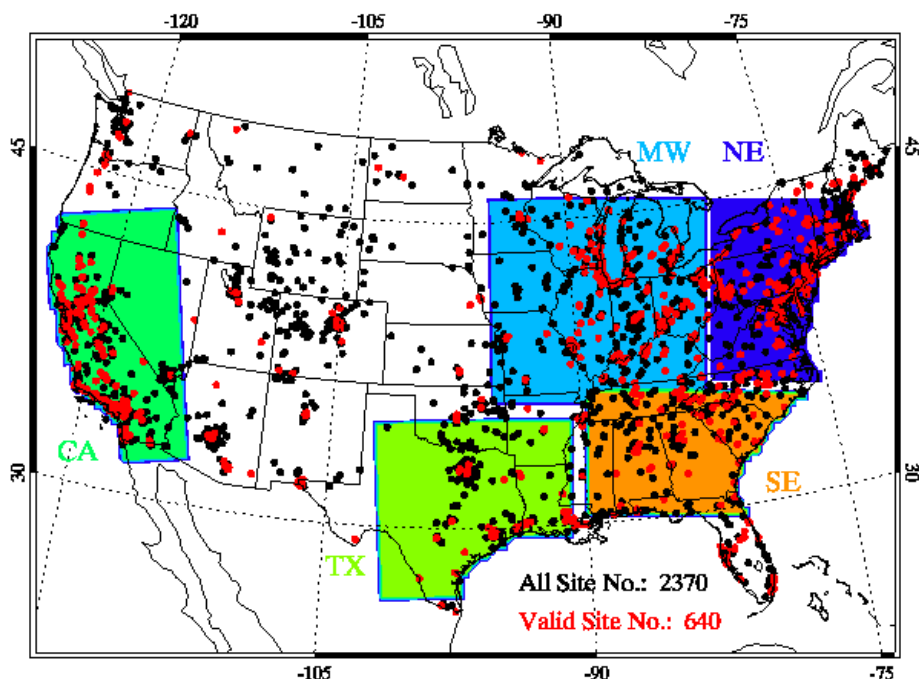


2002	0.56	0.77	-14.1	9.5	2010	0.69	0.75	-7.8	5.1
2003	0.65	0.77	-0.7	4.7	2011	0.84	0.62	-13.5	8.2
2004	0.81	0.59	3.2	4.4	2012	0.62	0.73	-9.4	6.1
2005	0.54	0.64	-8.8	6	2013	0.74	0.70	7.0	4.1
2006	0.74	0.60	-14	9	2014	0.84	0.40	0.9	4.0
2007	0.56	0.71	-14.1	9	2015	0.71	0.44	-2.6	4.2
Northeast									
2000	0.50	0.25	7.9	7.0	2008	0.46	0.11	-0.5	5.8
2001	0.46	0.28	-3.6	6.0	2009	0.67	0.23	13.7	7.3
2002	0.51	0.13	-8.5	8.3	2010	0.49	0.10	-0.4	5.6
2003	0.85	0.16	3.0	5.3	2011	0.47	0.31	3.2	5.9
2004	0.81	0.21	10.0	6.6	2012	0.55	0.17	-2.9	5.3
2005	0.84	0.11	2.5	5.8	2013	0.78	0.45	11.6	6.4
2006	0.45	0.21	3.0	6.0	2014	0.60	0.33	-4.8	5.1
2007	0.48	0.19	-0.7	5.6	2015	0.49	0.11	2.2	5.1
Midwest									
2000	0.41	0.25	3.4	5.9	2008	0.44	0.25	3.5	4.7
2001	0.55	0.30	-2.3	4.9	2009	0.54	0.22	14	7.2
2002	0.45	0.27	-5.2	7.0	2010	0.57	0.12	2.4	5.3
2003	0.66	0.25	-0.1	4.7	2011	0.45	0.21	1.1	5.6
2004	0.68	0.44	13.9	7.5	2012	0.46	0.19	-11.6	8.3
2005	0.76	0.15	-4.4	5.6	2013	0.74	0.18	4.9	4.0
2006	0.50	0.17	0.3	5.0	2014	0.64	0.20	5.7	4.1
2007	0.39	0.20	-0.6	5.6	2015	0.68	0.27	8.7	4.7

651 NMB: Normalized Mean Bias (Unit: %)
 652 RMSE: Root Mean Square Error (Unit: ppbv)
 653



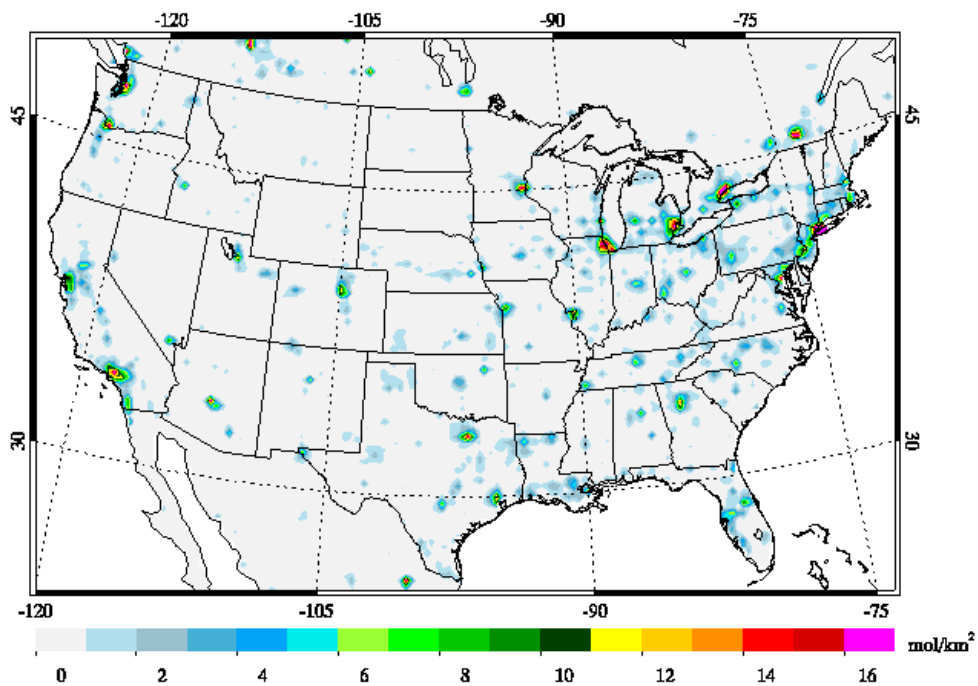
654 **Figure 1.** Locations of EPA AQS sites for surface ozone monitoring during 1990-2015. Red dots
655 stand for monitoring sites with more than 20 year record. Black dots show the locations of
656 monitoring sites have short data records which are not used in this study. The map shows the
657 CWRf-CMAQ 30-km domain and five subdomains sensitive to air pollution. CA: California
658 (including nearby parts of Nevada, Arizona and Oregon); TX: Texas (including nearby parts of
659 Louisiana, Arkansas, and Oklahoma); SE: Southeast; NE: Northeast; MW: Midwest. Please note
660 that our CA and TX subdomains include more area than the states of California and Texas.



661



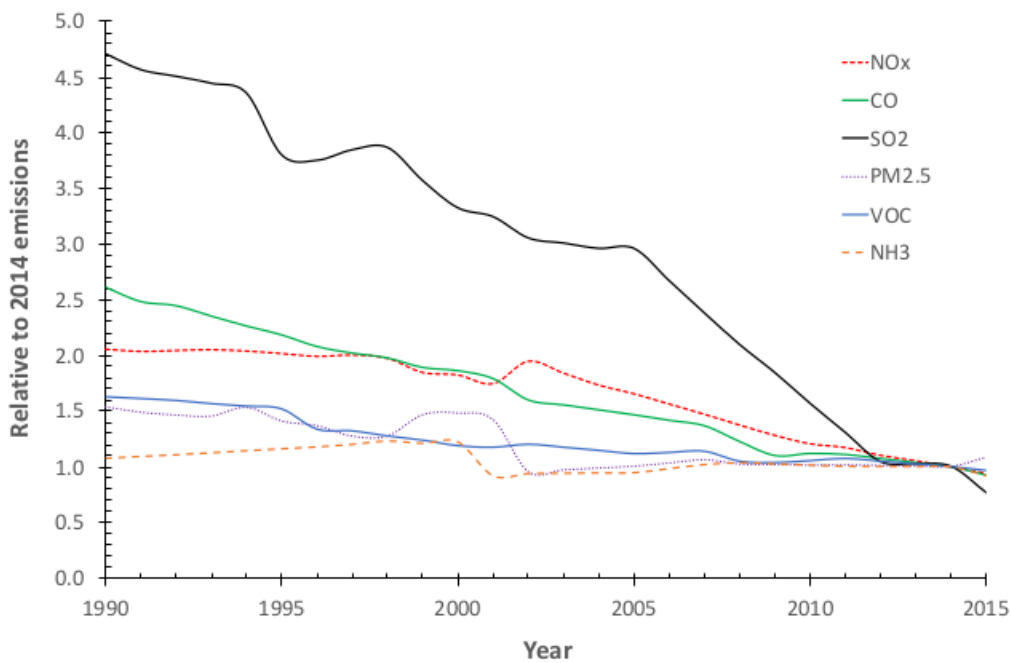
662 **Figure 2.** Averaged daily NO_x emissions between 2010 and 2015 in the modeling domain (Unit:
663 mol/km^2 per second).



664



665 **Figure 3.** Anthropogenic emission evolution relative to 2014 in the modeling domain from 1990
666 – 2015.

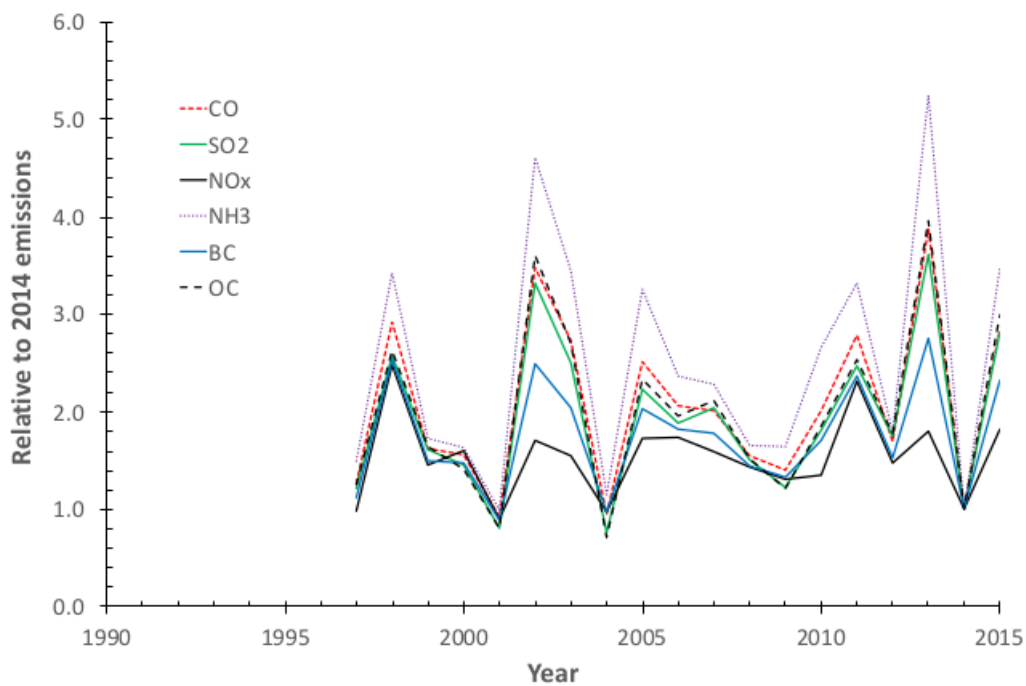


667

668



669 **Figure 4.** Fire emission evolution relative to 2014 in the modeling domain from 1990 – 2015.
670 Noting that GFED fire emissions are not available before 1997.

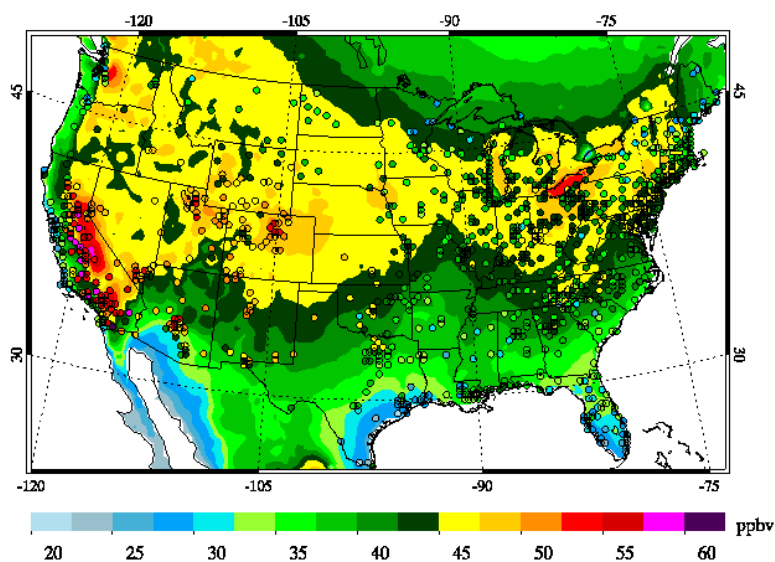


671

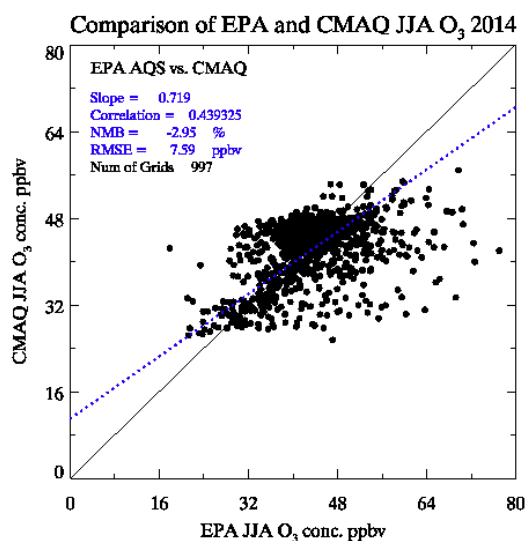


672 **Figure 5.** Comparison of summer MDA8 ozone concentrations from EPA AQS observations and
673 CMAQ simulations in 2014. AQS station data were gridded to the CMAQ grid using the EPA
674 RSIG software. a) Contour plot, the background stands for the CMAQ outputs and the dots stand
675 for gridded AQS observations; b) Scatter plot of the gridded AQS observations and co-located
676 CMAQ outputs.

677 a)



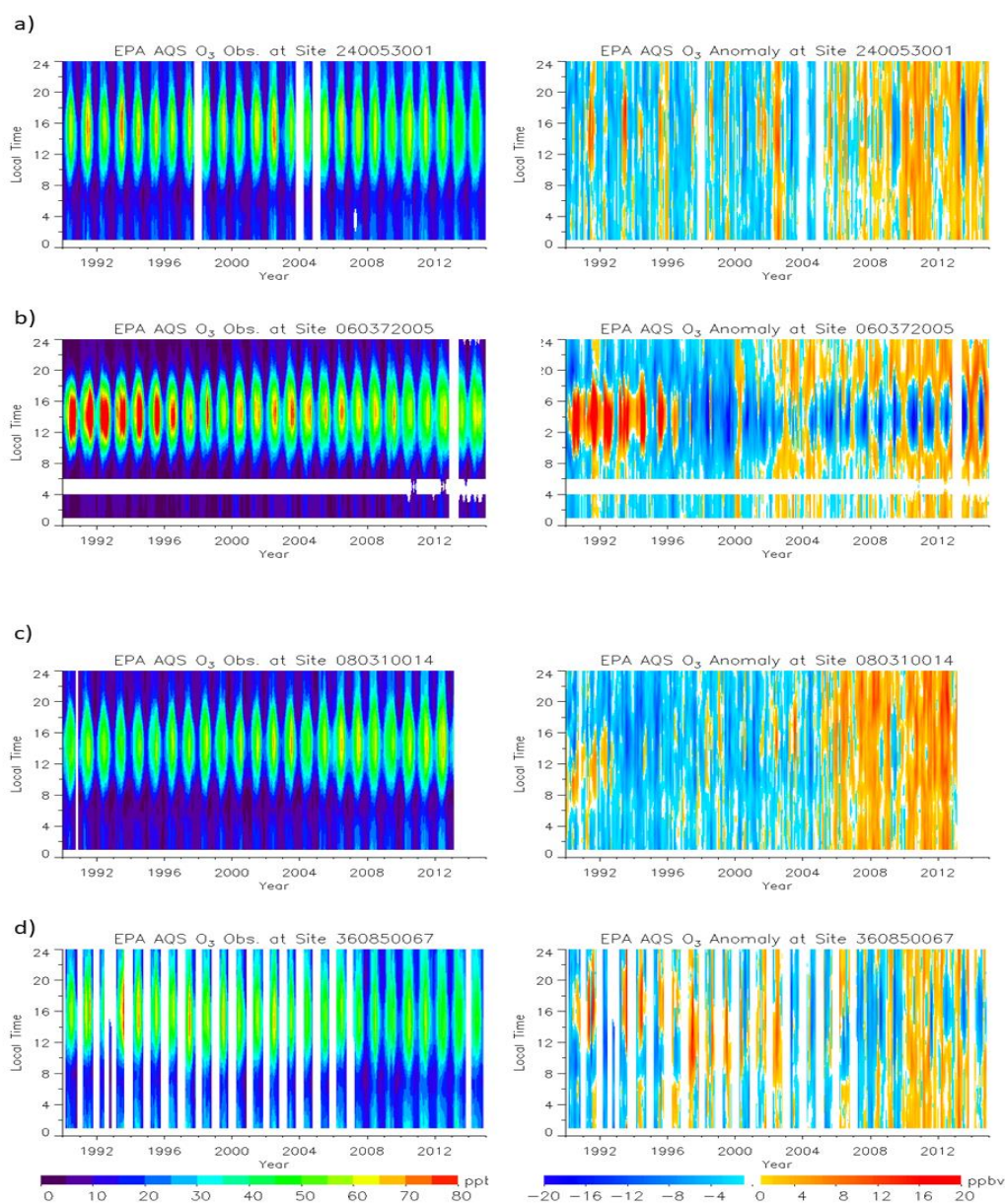
678
679 b)



680



681 **Figure 6.** The box-averaging analyses of AQS ozone observations at selected sites from 1990-
682 2015. a) Essex, Maryland (suburban Baltimore, AQS ID 240053001); b) Pasadena, California
683 (downtown Los Angeles, AQS ID 060372005); c) Denver, Colorado (downtown Denver, AQS ID
684 080310014); d) Staten Island, New York (suburban New York City, AQS ID: 360850067). Left
685 column shows the monthly mean, right column shows the anomaly values. White patches stand
686 for missing data or not sufficient data for the box-averaging analysis.

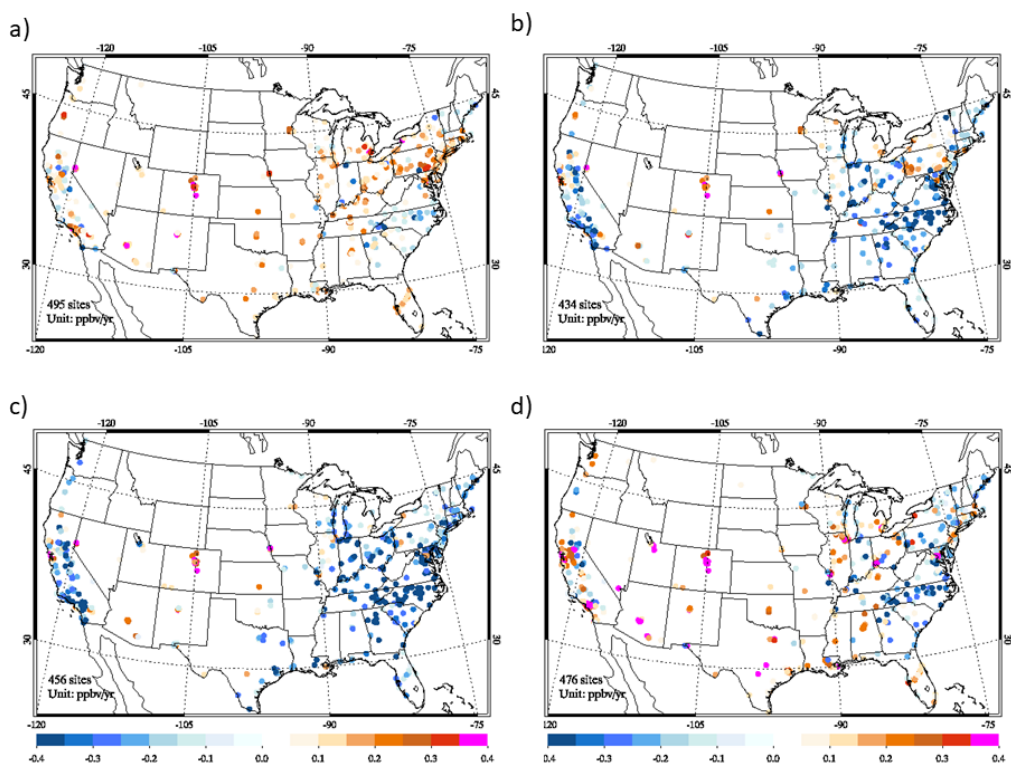


687

688



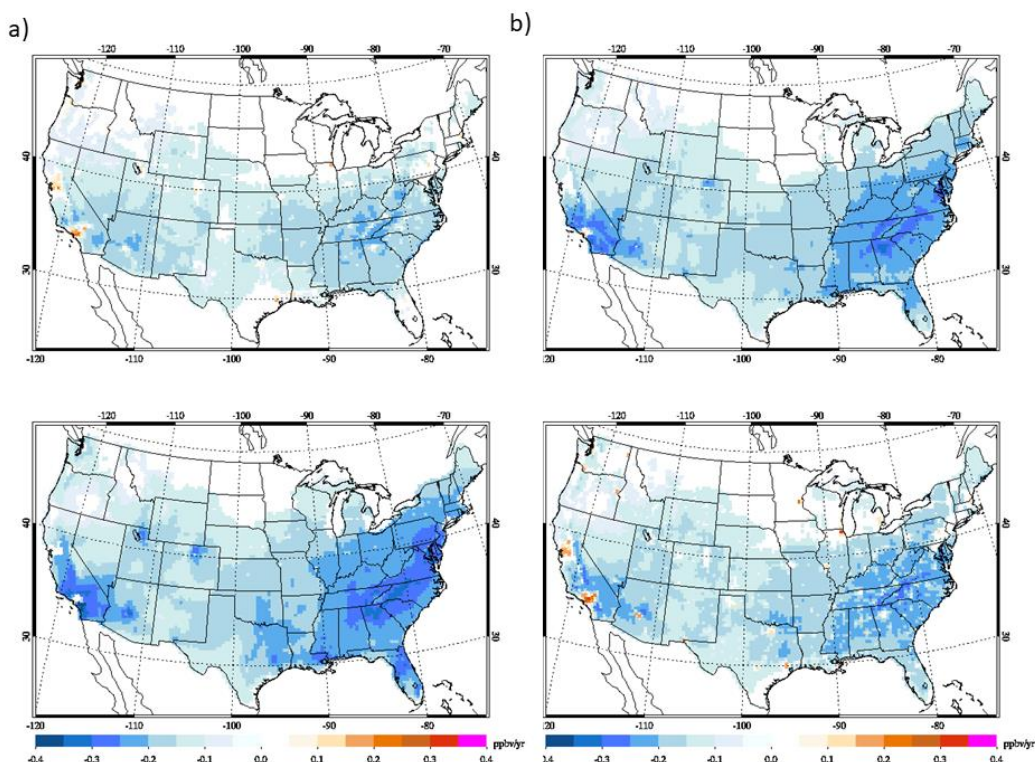
689 **Figure 7.** Trend in ozone observations at selected EPA AQS sites during 1990-2015 (Unit:
690 ppbv/yr). a) at 8 am; b) at 12 pm; c) at 4 pm; d) at 8 pm (all local time). We only show the sites
691 with statistically significant linear trend in the plots.



692



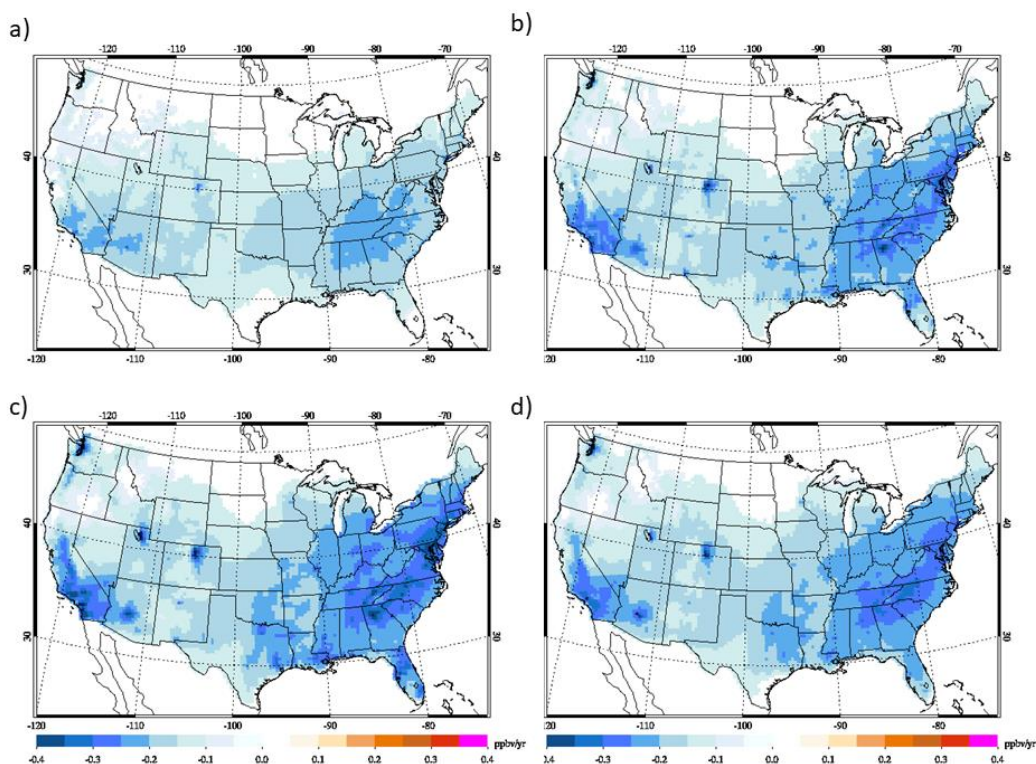
693 **Figure 8.** Trends in ozone simulations from CMAQ during 1990-2015 (Unit: ppbv/yr). a) at 8
694 am; b) at 12 pm; c) at 4 pm; d) at 8 pm (all local time). We only show CMAQ grids with
695 statistically significant linear trend in the plots.



696



697 **Figure 9.** Trend in O_x simulated by CMAQ during 1990-2015. a) at 8 am; b) at 12 am; c) at 4
698 pm; d) at 8 pm (all local time). We only show CMAQ grids with statistically significant linear
699 trend in the plots.

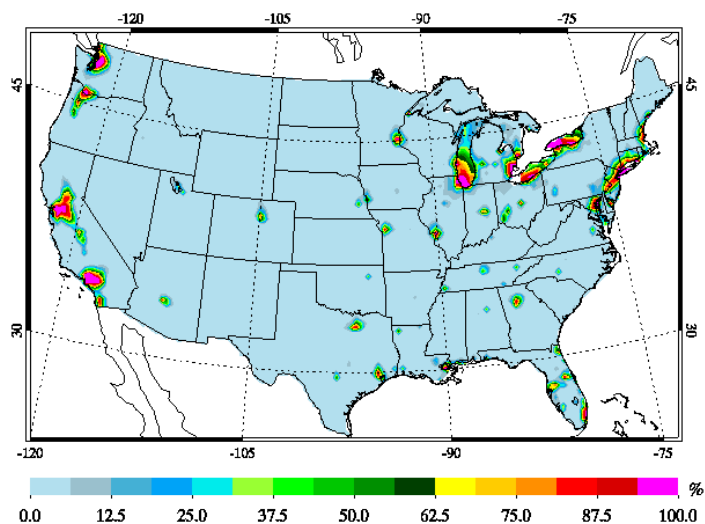


700



701 **Figure 10.** Probability of VOC-sensitive photochemical ozone production (i.e., $O_3/NO_y < 15$) in
702 the CONUS simulated by CMAQ at 2 pm local time in July, a) 1995; b) 2005; and c) 2015

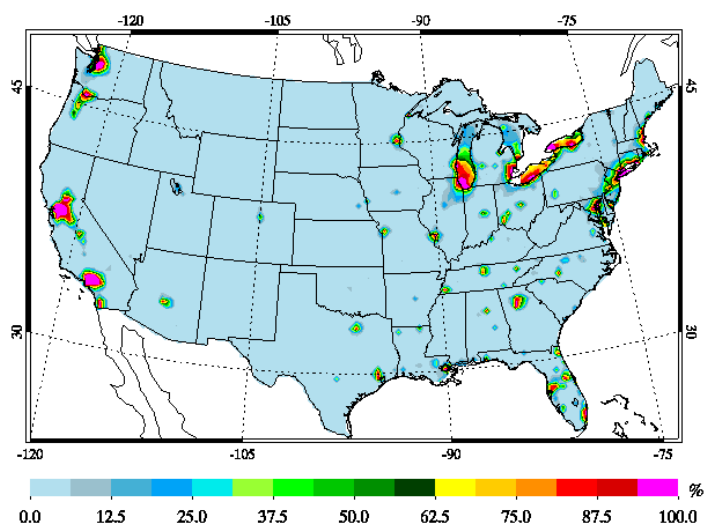
703 a)



704

705

706 b)

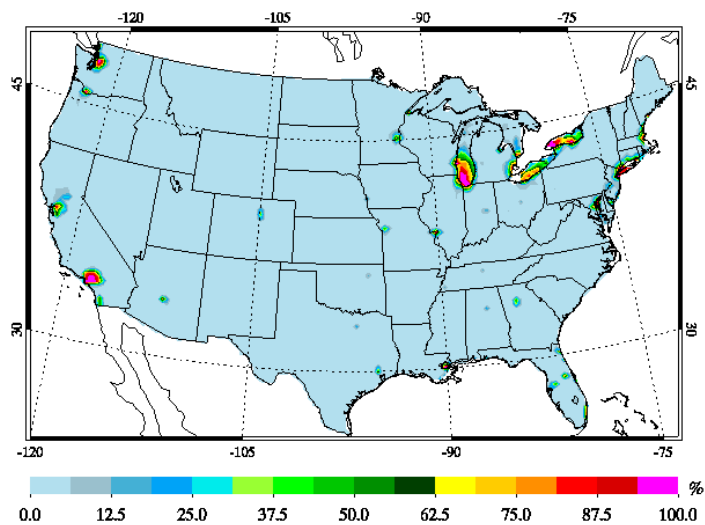


707

708



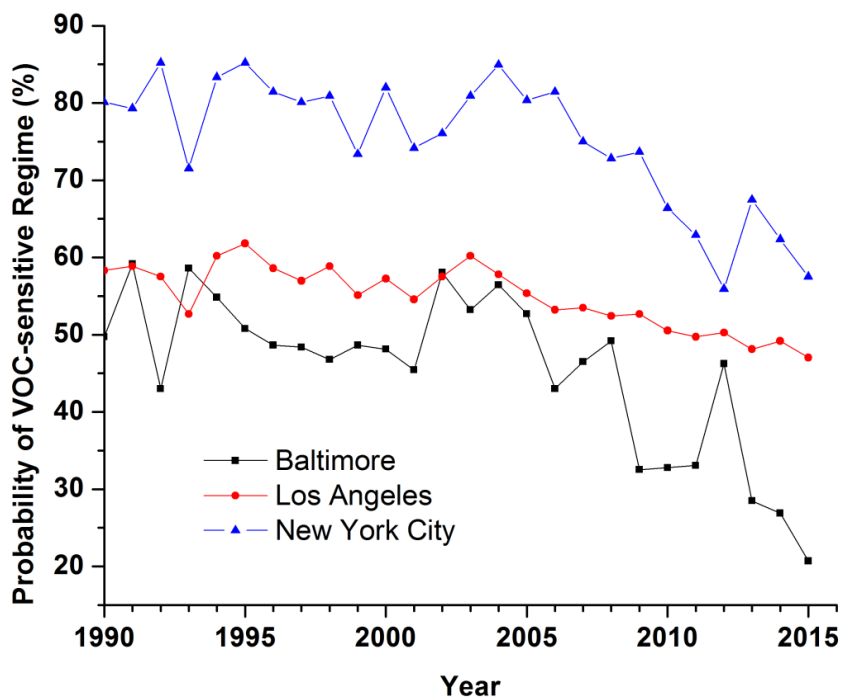
709 c)



710



711 **Figure 11.** Long-term trends in probability of VOC-sensitive photochemical production of
712 surface ozone in three major urban areas at 2 pm in July. Probability is calculated using averages
713 of 3×3 grids centered at downtown.



714